

Pressure Drop Distribution in Smooth and Rib Roughened Square Channel with Sharp 180° Bend in the Presence of Guide Vanes

Venkata Ratna Rao.D and S. V. Prabhu*

Department of Mechanical Engineering, Indian Institute of Technology, Bombay, India

An experimental investigation is carried out to study the effect of several turn treatments like single guide vane (short and long) and multiple guide vanes on the pressure drop distribution in smooth and rib roughened square channels with a sharp 180° bend. The sharp 180° turn is obtained by dividing a rectangular passage into two square channels using a divider wall with a rounded tip at the location where the flow negotiates the turn. In rib roughened channels, ribs are configured on the top and bottom surfaces in a symmetric arrangement with an angle of 90° to the mainstream flow. Rib height-to-hydraulic diameter ratio (e/D) is maintained constant at 0.14 with a constant pitch-to-rib height ratio (P/e) of 10. The pressure drop distribution normalized with the mainstream fluid dynamic pressure head is presented for the outer surfaces. Results suggest that 90° multiple guide vanes result in the decrease of overall pressure drop by around 40% in smooth square channels. However, a reduction in overall pressure drop by only 15% is achievable through guide vanes in rib roughened square channels.

Keywords 180° bend, Guide vane, Pressure loss, Gas turbine blade cooling passage, Friction factor

INTRODUCTION

In advanced gas turbine engine designs, increased speeds, pressures, and temperatures are used to increase thrust/weight ratios and to reduce the specific fuel consumption. Hence, the turbine blades are subjected to the loads resulting from the centripetal acceleration field of the order of 10^4 g, while simultaneously exposed to thermal environments hot enough to cause the blade material to glow red (Metzger et al., 1984). High pressure

air from the compressor introduced through the hub section into the blade interior helps in cooling the blade and keeping the blade material below the metallurgically permissible temperature limits. The cooling air flows through a complicated serpentine passage inside the blade that comprises of several channels along the blade height with the adjacent channels connected by sharp 180° bends. Many other applications such as the hot gas manifold of the space shuttle main engine power head (Kwak, 1986) and ventilation piping systems (Liou, 1999) involve two adjacent ducts connected by a 180° bend. The space constraints in coolant blade passages dictate a small radius of curvature for the 180° turn, often smaller than the hydraulic diameter. Flow fields in such sharp 180° bends comprise of the turning geometry: induced secondary flow, flow separation, re-circulation, and reattachment. This results in noticeable effects on the pressure loss and non-uniformity in heat transfer distributions (Liou, 1999). Hence, the design of the cooling passages involving sharp 180° bends requires detailed knowledge of the flow resistances offered by the cooling passages. Local and overall distribution of the pressure drop through the passages determines the total coolant flow rate that can be allowed through the coolant passage for a given supply pressure. The objective of the designer is to reduce the overall pressure drop so that coolant flow rate through the passage increases, resulting in improved convection heat transfer coefficients.

Metzger et al. (1984) studied the effects of channel geometry such as the before-turn and after-turn channel aspect ratio, the turn clearance, and flow Reynolds number on the pressure drop distribution. They concluded that both the channel aspect ratio and turn clearance have an important influence on the pressure drop characteristics of two-pass smooth rectangular channels. Liou et al. (1999) investigated the effect of divider wall thickness on the fluid flow in a two-pass smooth square duct with a 180° straight corner turn. They found that the divider wall thickness has profound effects on the flow features inside and immediately after the turn. They observed that the turbulence level and uniformity in the region immediately after the turn decrease and increase with the increasing divider wall thickness.

Received 18 February 2003; in final form 10 September 2003.

*Corresponding author. Tel.: +91 22-25767515, Fax: +91 22-25723480. E-mail: svprabhu@me.iitb.ac.in

Son et al. (2002) carried out Particle Image Velocimetry (PIV) experiments to measure the detailed average velocity distributions and turbulent kinetic energy for both the main and secondary flows in a two-pass square channel with a smooth wall and a 90° rib roughened wall. PIV measurement results were compared with the heat transfer experimental data of Ekkad and Han (1997). Their study indicates that the flow impingement is the primary factor for the two-pass square channel heat transfer enhancement rather than the flow turbulence level itself.

Han and Zhang (1989) investigated the combined effects of flow channel aspect ratio and the sharp 180° bend ($W/D = 0.25$) on the distribution of the local pressure drop in a stationary three-pass channel for both smooth and rib roughened channels. Metzger and Plevich (1990) conducted an experimental study to evaluate the effect of geometric turn region inserts on pressure losses for flow through a sharp 180° channel with 90° ribs. Various turn region treatments studied include corner fillets, radial ribs, and turning vanes. The results show that the inclusion of turning vane reduces the pressure drop losses associated with the coolant flows through sharp 180° turns. Venkata Ratna Rao et al. (forthcoming) conducted an experimental investigation to study the effect of several turn treatments like single guide vane (short and long) and multiple guide vanes on the pressure drop distribution in a square cross sectioned smooth channel with a sharp 180° bend. They observed that properly shaped 180° vanes located in the center of the bend decrease the overall pressure drop by as much as 40–45% compared to the no-guide vane situation. This study is limited to smooth square channels with blunt

ended sharp 180° bend configuration only. Typical gas turbine blade coolant passages as shown in Figure 1 consist of both blunt and round ended sharp 180° bend. There is no information on the effect of the turn treatments on the pressure drop distribution in smooth and rib roughened square channels with round ended sharp 180° bends in the open literature. The main objective of the present work is to study the effect of single- (short and long) guide vane and multiple guide vanes of different configurations placed at different locations within the bend on the local and overall pressure drop distributions in a two-pass square smooth and rib roughened passages with a round ended sharp 180° bend.

EXPERIMENTAL SET-UP AND PROCEDURE

Smooth Channel

A schematic diagram of the experimental set-up is shown in Figure 2. Water is used as the working medium and a large rectangular tank of about 200 liter capacity serves as a storage reservoir. Water is pumped into the test section from the tank by a 0.4 kW centrifugal pump. Water flowing through the test section is recirculated to the tank. Gate valve 'G2' is used to adjust the volume flow rate of the water supplied to the test-section. Measurement of the volume flow rate is carried out by a rotameter 'R' placed upstream of the test section. The test section is manufactured from a 0.0078 m-thick perspex sheet cut, machined, and chemically bonded to form a channel of 0.029 m square cross-section and 1.2 m length. A three-dimensional view of the test section is shown in Figure 3. Divider wall of thickness (W) 0.0058 m is used. The pressure drop is measured by a stationary U-tube differential manometer with carbon-tetrachloride as the manometric fluid. Figure 4 shows the static pressure tap locations on the outer surface.

Several turn treatments chosen for guiding the flow within the bend include short guide vane, long guide vane, and multiple

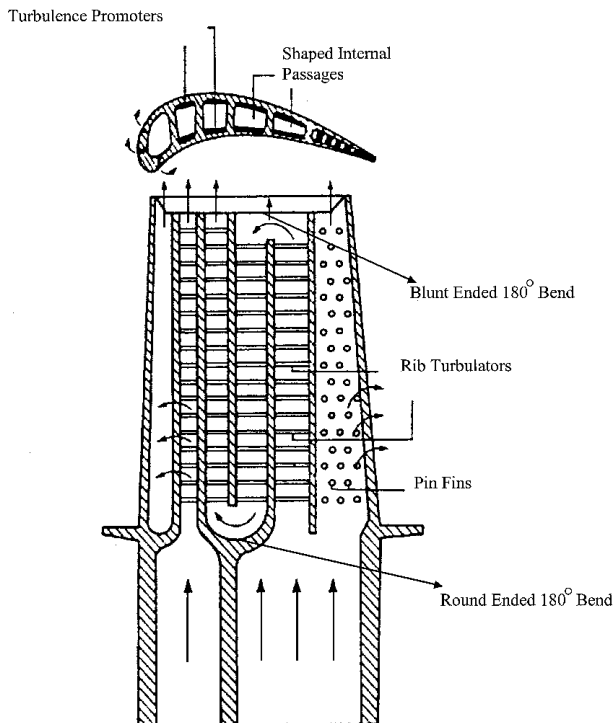
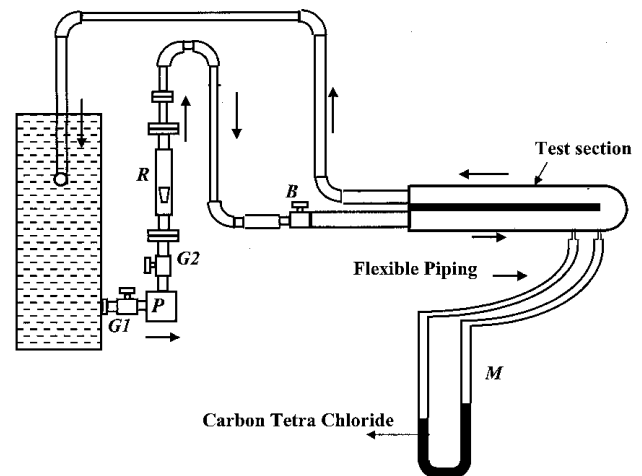


FIGURE 1

Typical multipass turbine blade (Han and Zhang, 1989).



G1: G2; Gate valve; B: Ball valve; P: Pump; R: Rotameter; M: Manometer

FIGURE 2

Schematic of the experimental set-up.

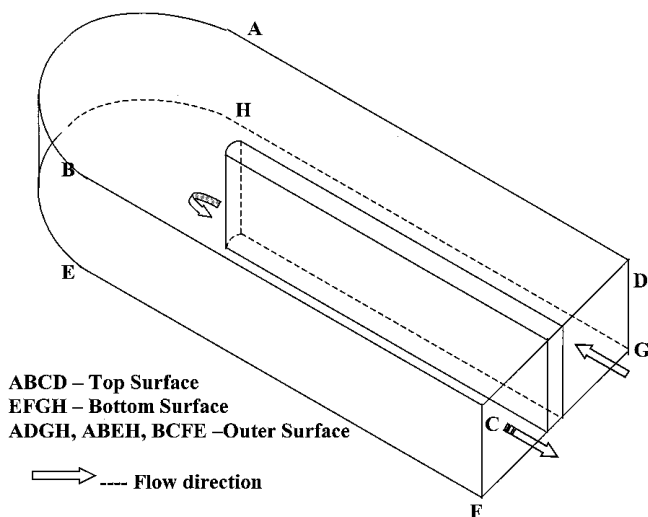


FIGURE 3
Three-dimensional view of the test section.

guide vanes. Details of the configurations used in smooth channel are given in Figure 5 and Table 1.

Figures 6 and 7 show the dimensions of the short and long guide vane configuration made of perspex sheet. Short and long guide vanes are placed in different locations within the bend region and corresponding cases include 1 and 6 (short guide vane) and cases 2, 3, 4, and 5 (long guide vane). 90° and 180° mild steel vanes of 14.5 mm radius (Figure 8) are placed along each diagonal of the bend as in Case 7 (Figure 5). 3 95° mild steel vanes of 9.8 mm radius (Figure 9) are placed along each diagonal of the bend as in Case 8 (Figure 5). 4 95° mild steel vanes of 9.8 mm radius (Figure 9) are placed along each diagonal of the bend as in Case 9 (Figure 5). 2 extended 180° guide vanes with radii of curvature of 12 mm and 22 mm (Figure 10) are placed within the bend as in Case 10. 90° and 180° extended guide vane of 14.5 mm radius (Figure 11) are placed within the bend as in Case 11.

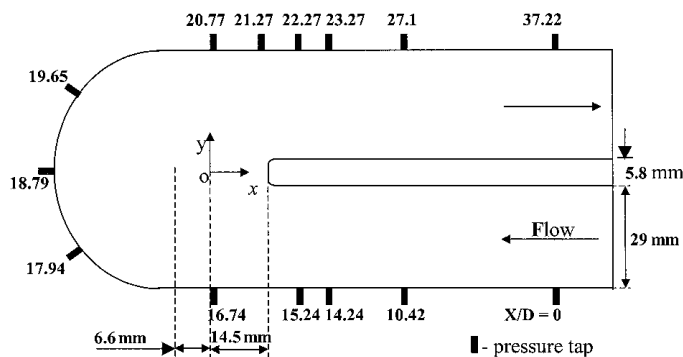


FIGURE 4
Schematic of the 180° bend indicating the pressure tap locations on the outer surface of smooth channel.

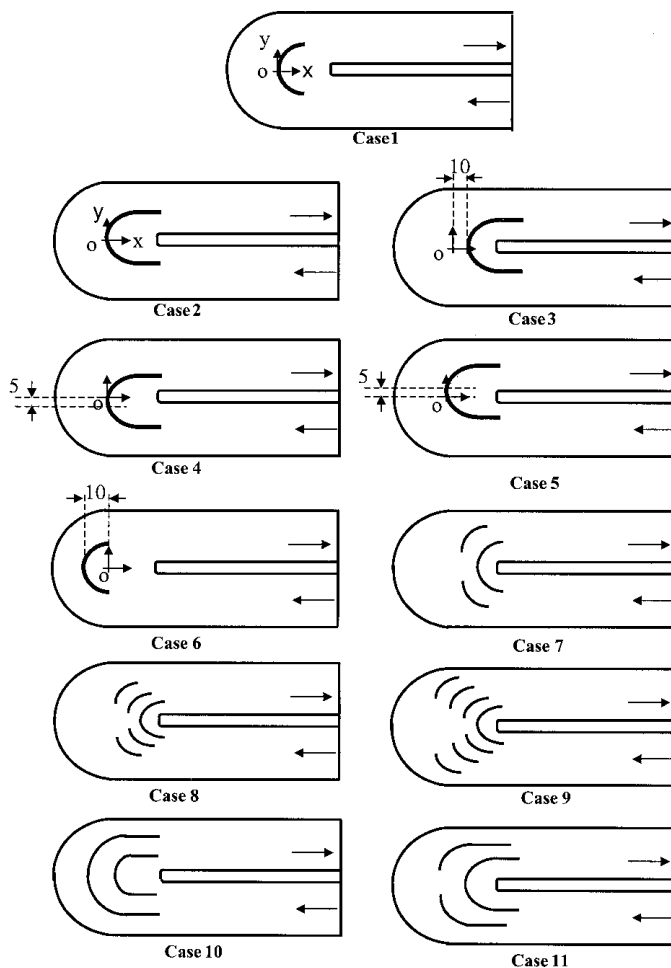


FIGURE 5
Several test cases covered in this study for smooth passage test section.

Rib Roughened Channel

The test section is manufactured from a 0.0078 m-thick perspex sheet cut, machined, and chemically bonded to form a channel of 0.028 m square cross-section and 1.2 m length. A divider wall of thickness (W) 0.0058 m is used. Plexiglas ribs of 0.028 m length with a 0.004 m \times 0.004 m cross section are glued periodically on the top and bottom surfaces of the test section. The ribs on the two surfaces are symmetric with respect to each other. The rib height-to-hydraulic diameter ratio (e/D) of 0.14 with a constant pitch-to-rib height ratio of (P/e) of 10 is tested. The ribs are placed at an angle of 90° to the mainstream flow. There are no ribs in the turn region. Figure 13 shows the ribs arrangement and static pressure tap locations on the outer surface of the ribbed test section. The total number of ribs on each of the top and bottom surfaces of the upstream/downstream channel are 14.

Several turn treatments chosen for guiding the flow within the bend include short guide vane, long guide vane, and multiple

TABLE 1
Turn Region Treatments with Smooth Channels (Details in Figure 5)

Case	Description
1	Short guide vane placed at the center of the bend (at origin 'o').
2	Long guide vane placed at the center of the bend (at origin 'o').
3	Long guide vane shifted towards divider tip by 10 mm (in the negative x -direction) from the center of the bend.
4	Long vane shifted towards upstream by 5 mm (in the positive y -direction) from the center of the bend.
5	Long guide vane shifted towards downstream by 5 mm (in the negative y -direction) from the center of the bend.
6	Short guide vane shifted towards end surface by 10 mm (in the negative x -direction) from the center of the bend.
7	Guide vane of 90° included angle with 14.5 mm radius—2 along each diagonal of the bend.
8	Guide vane of 95° included angle with 9.8 mm radius—3 along each diagonal of the bend, not equally spaced.
9	Guide vane of 95° included angle with 9.8 mm radius—4 along each diagonal of the bend, equally spaced.
10	Two guide vanes of 180° included angle with radii of curvature 12 mm and 22 mm, equally spaced.
11	Equally spaced 180° extended vane and two 90° extended vanes.

guide vanes. Details of the configurations used in the rib roughened channel are given in Figure 14 and Table 2. Figures 6 and 7 show the dimensions of the short and long guide vane configuration made of perspex sheet. Short and long guide vanes are placed at the center of the bend region and corresponding cases include 2 (short guide vane) and 3 (long guide vane). 90° and 180° mild steel vanes of 14.5 mm radius (Figure 8) are placed along each diagonal of the bend as in Case 4 (Figure 14). 90° and 180° extended guide vane of 14.5 mm radius (Figure 11) are placed within the bend as in Case 5. 4 95° mild steel vanes of 9.8 mm radius (Figure 9) are placed along each diagonal of the bend as in Case 6 (Figure 5). 3 95° mild steel vanes of 9.8 mm radius (Figure 9) are placed along each diagonal of the bend as in Case 7 (Figure 5). 2 extended 180° guide vanes with radii of curvature of 12 mm and 22 mm (Figure 10) are placed within the bend as in Case 8.

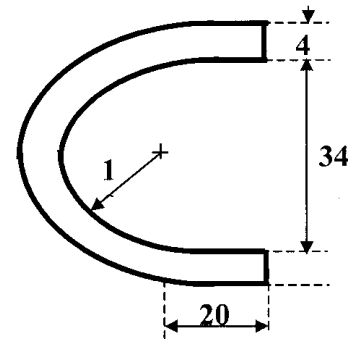


FIGURE 7

Long guide vane (Case 2, 3, 4, and 5 in smooth channel; Case 3 in rib roughened channel).

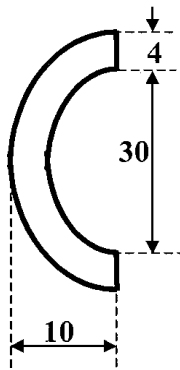


FIGURE 6

Short guide vane (Case 1 and 6 in smooth channel; Case 2 in rib roughened channel).

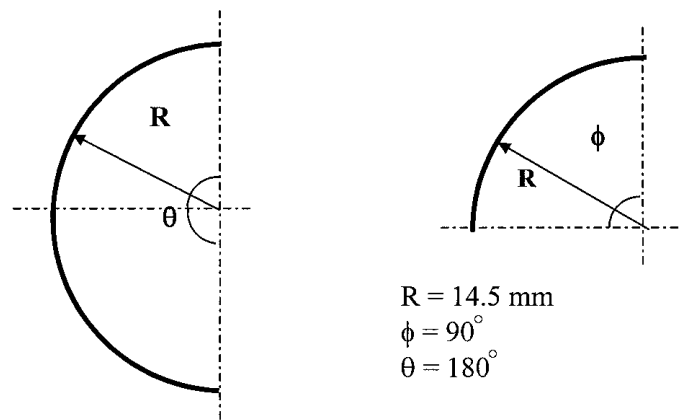


FIGURE 8

90° and 180° vanes (Case 7 in smooth channel; Case 4 in rib roughened channel).

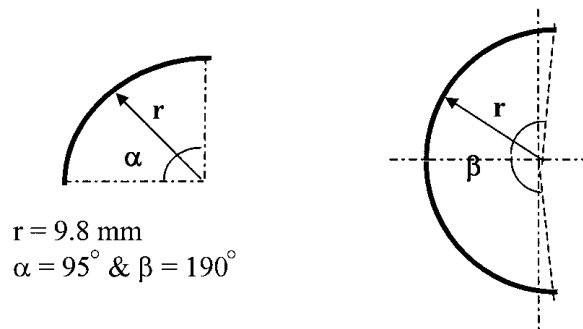


FIGURE 9

95° and 190° vanes (Case 8 and 9 in smooth channel; Case 6 & 7 in rib roughened channel).

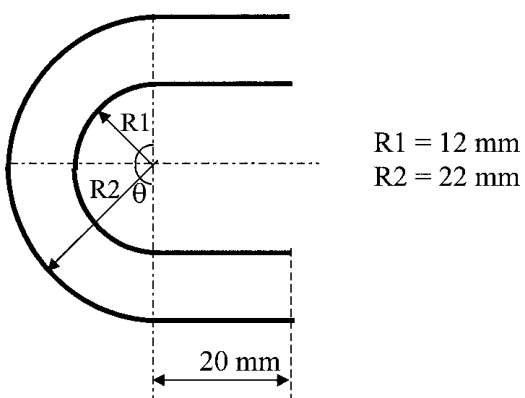
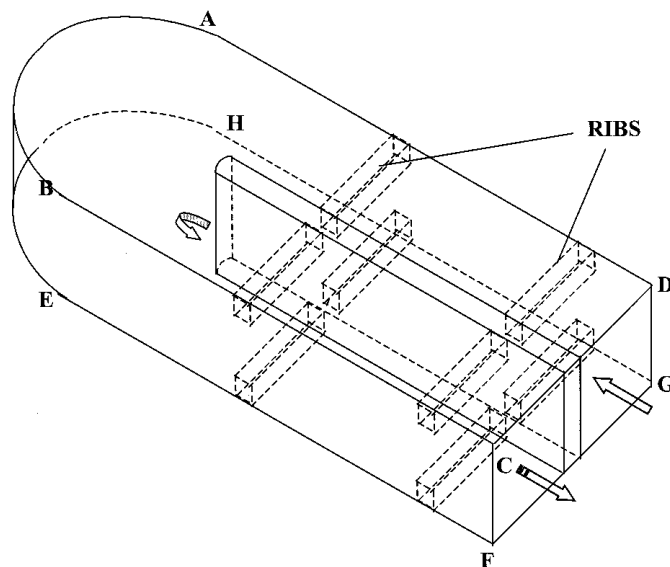


FIGURE 10

180° extended vanes (Case 10 in smooth channel; Case 8 in rib roughened channel).

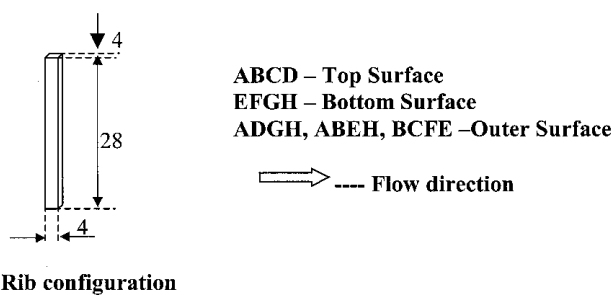


FIGURE 12

Three-dimensional view of the test section.

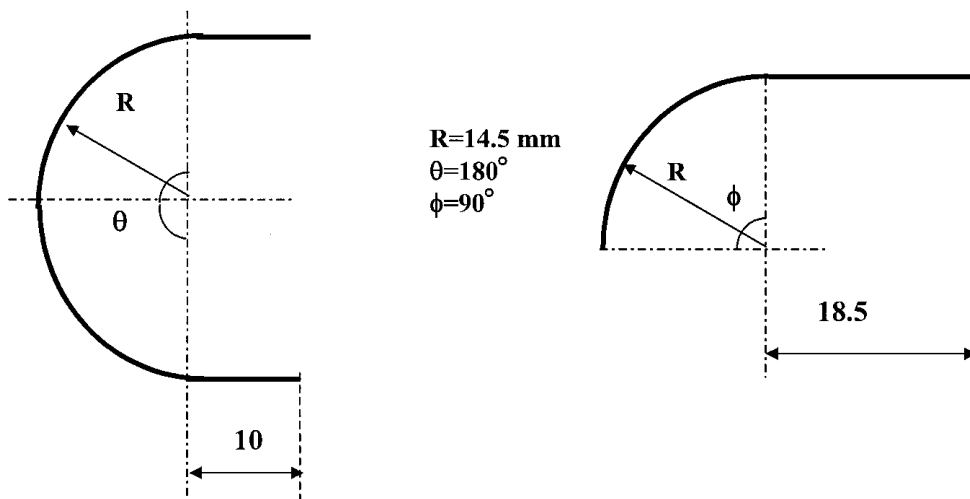


FIGURE 11

90° and 180° extended vanes (Case 11 in smooth channel; Case 5 in rib roughened channel).

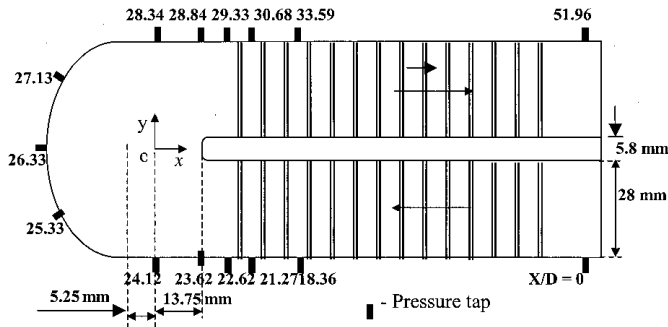


FIGURE 13

Schematic of the sharp cornered 180° bend indicating the pressure tap locations on outer surface of rib roughened test section.

DATA REDUCTION

The local pressure drop is non-dimensionalized by normalizing with the mainstream fluid dynamic pressure head as

$$K = \frac{P_x - P_{in}}{\left(\frac{1}{2}\right)\rho U^2} \quad [1]$$

The overall mean pressure drop is the calculated difference between the arithmetic average values of pressure drop on all the four surfaces (top, bottom, and twice the outer surface) at the channel entrance and the channel exit of the test section. This overall pressure drop is used to calculate the average friction factor given by

$$f = \frac{P_{ex} - P_{in}}{\left(\frac{1}{2}\right)\rho U^2 \left(4\frac{L}{D}\right)} \quad [2]$$

For smooth channels cases, the length 'L' is equal to 37.22 times hydraulic diameters which include the bend and equal portions of the straight channel upstream and downstream of the bend. For rib roughened channels cases, the length 'L' is equal to 51.96 hydraulic diameters which includes the bend and equal portions of the straight channel upstream and downstream of the bend. The average friction factor is normalized by

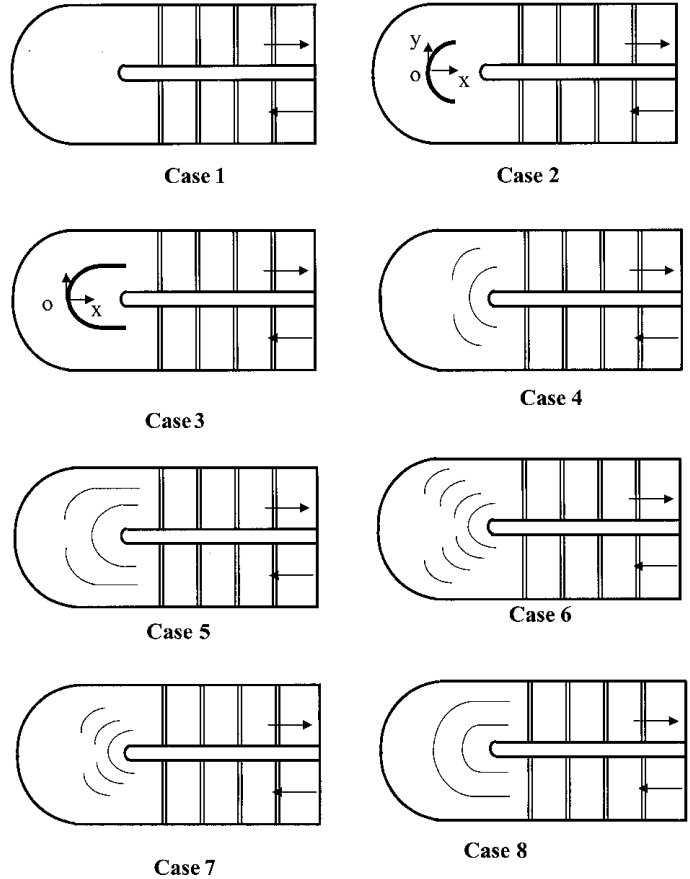


FIGURE 14

Several test cases covered in this study for smooth passage test section.

the friction factor for fully-developed turbulent flow in smooth circular tubes ($10000 \leq Re \leq 100000$) proposed by Blasius ($f/f(FD) = f/(0.046Re^{-0.2})$). Uncertainties in parameters are estimated by using the root-sum-square method of Kline and McClintock (1953) and Taylor (1997). The measured quantity and its uncertainty can be expressed as $R = R \pm \delta R$. The overall uncertainty assigned to a given measurement is the root sum

TABLE 2
Turn Region Treatments with Rib Roughened Channels

Case	Description
1	Without guide vane in the bend (base case).
2	Short guide vane placed at the center of the bend (at origin 'o').
3	Long guide vane placed at the center of the bend (at origin 'o').
4	Guide vane of 90° included angle with 14.5 mm radius—2 along each diagonal of the bend.
5	Equally spaced on 180° extended vane and two 90° extended vanes.
6	4 equally spaced vanes of 95° included angle with 9.8 mm radius along each diagonal of the bend (7 mm apart).
7	3 equally spaced vanes (as in the Case 9) of 95° included angle with 9.8 mm radius along each diagonal of the bend (7 mm apart).
8	2 guide vanes of 180° included angle with radii of curvature 12 mm and 22 mm which are equally spaced (11 mm apart).

square combination of the fixed error due to the instrumentation and the random error observed during the running trials. The uncertainties of flow rate, hydraulic diameter, pressure drop, length of the test section, velocity of the flow, and average friction factor are estimated within $\pm 1\%$, $\pm 1\%$, $\pm 2\%$, $\pm 0.03\%$, $\pm 2.25\%$, and $\pm 6\%$, respectively.

RESULTS AND DISCUSSIONS

Smooth Square Channel with Sharp 180° Bend

Figure 15 shows the local pressure drop distribution of the outer surface of a bend with a W/D ratio of 0.2 for Reynolds numbers of 13,500 and 17,000. Pressure drop distribution indicates several flow features of the turn flow: separated flow regions in the upstream of the bend ($X/D = 15.24-16.74$) and along the downstream side of the divider rib ($X/D = 22.27-23.27$), radial inward wall surface accelerating flow within, and downstream of the divider tip ($X/D = 20.77-22.27$). This pressure drop distribution is in line with the pressure distribution and flow visualizations observed by Metzger et al. (1984).

Figure 16 shows the effect of short and long guide vanes located at the center of the bend on the pressure drop distribution. It can be seen that the overall pressure drop decreases by the presence of both short and long guide vanes by around 28–30%. The decrease in the overall pressure drop for both short and long guide vanes is nearly the same. The adverse pressure gradients on the upstream portion of the bend ($X/D = 15.24-16.74$) are decreased in short guide vane case and increased in

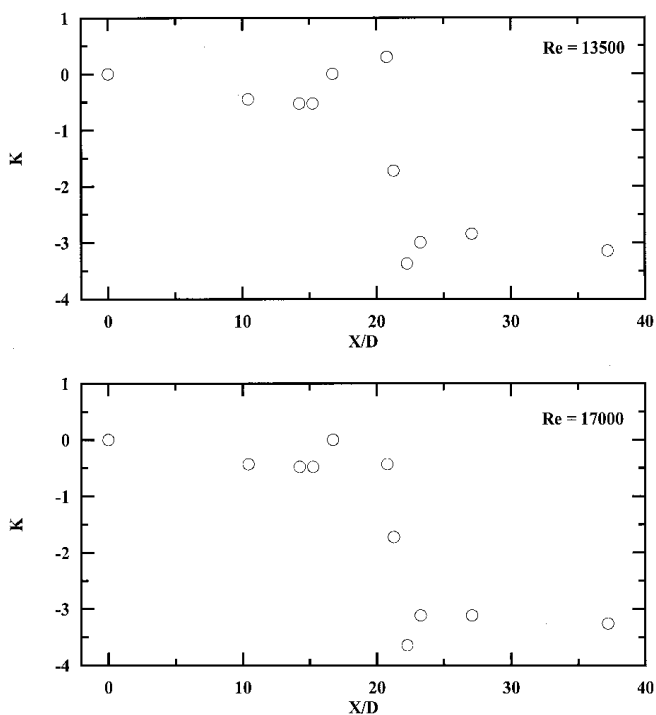


FIGURE 15

Outer surface pressure drop distribution in smooth square channel without guide vane in the bend region (base case).

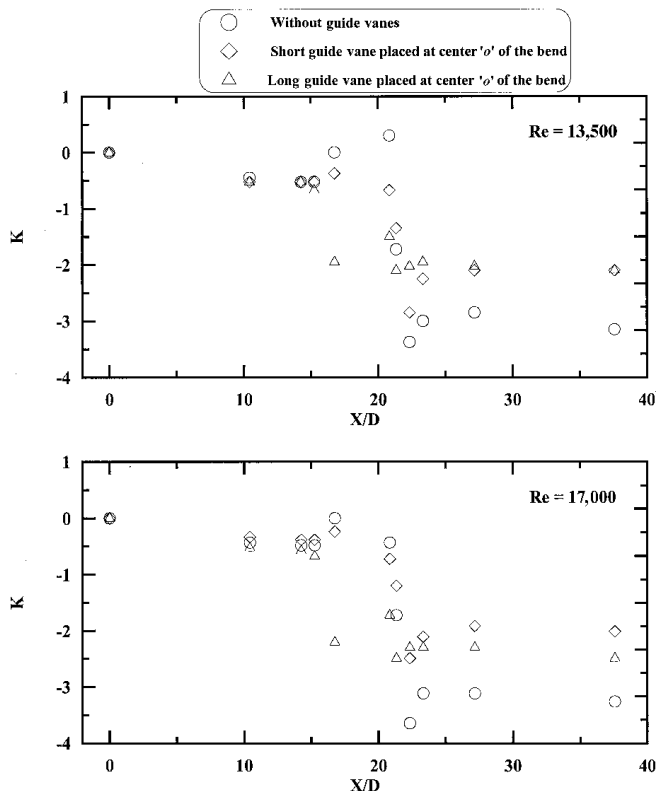


FIGURE 16

Outer surface pressure drop distribution in smooth square channel with short and long guide vane at the center of the bend.

long guide vane case when compared with the no-guide vane situation. Figure 17 shows the effect of shifting the short guide vane shifted towards the end surface by 10 mm on the local pressure drop distribution. The overall pressure drop decreases by placing the short guide vane at the center of the short guide vane being shifted towards the end surface. However, the decrease in the overall pressure drop is large in case of the short guide vane placed at the center of the bend. Figure 18 shows the effect of placing the long guide vane at various locations within the bend region. It can be observed that shifting the long guide vane towards the upstream and downstream surface increases the overall pressure drop. Shifting the long guide vane towards the divider tip results in the decrease in the overall pressure drop. However, the overall pressure drop is least when the long guide vane is placed at the center of the bend.

Figures 19, 20, 21, and 22 show the effect of multiple guide vanes of different configurations on the local pressure drop distribution. Figure 19 shows the effect of placing 14.5 mm radius of curvature for 2 guide vanes and 9.8 mm radius of curvature for 3 guide vanes on the local pressure drop distribution. The overall pressure drop decreases by placing the multiple guide vanes in the bend. Adverse pressure gradient zones continue to exist both in the upstream and downstream corner of the bend even in the presence of multiple guide vanes.

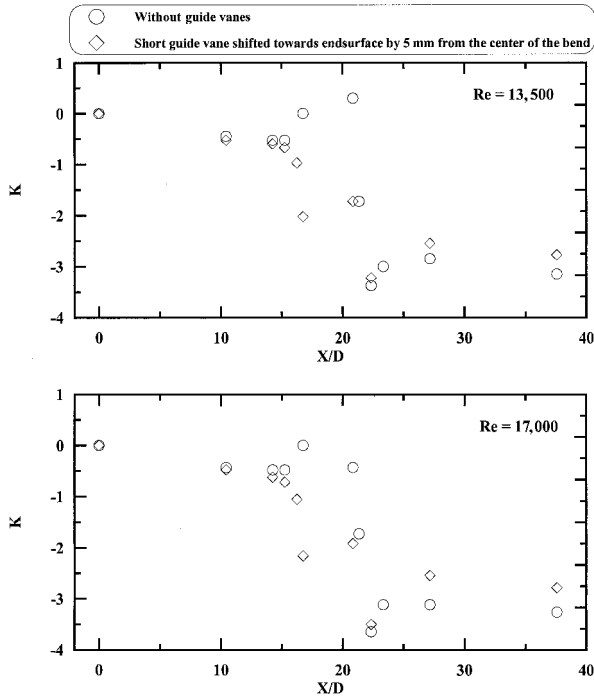


FIGURE 17

Outer surface pressure drop distribution in smooth square channel with short guide vane shifted from the center of the bend towards the endsurface.

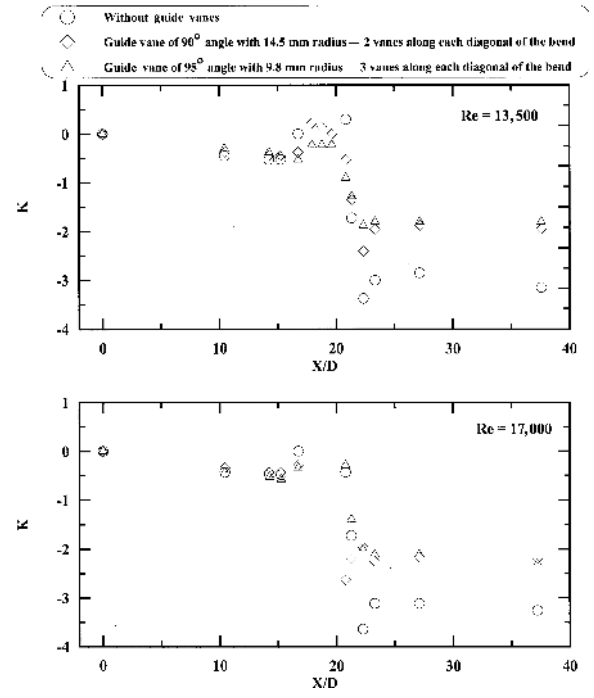


FIGURE 19

Outer surface pressure drop distribution in smooth square channel with 14.5 mm radius for 2 guide vanes (90° included angle) and 9.8 mm radius for 3 guide vanes (95° included angle).

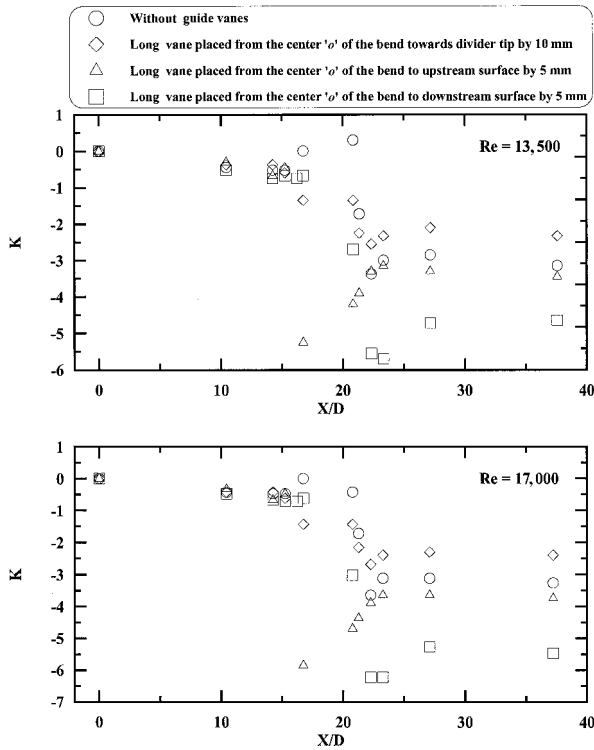


FIGURE 18

Outer surface pressure drop distribution in smooth square channel with long guide vane at different locations in the bend.

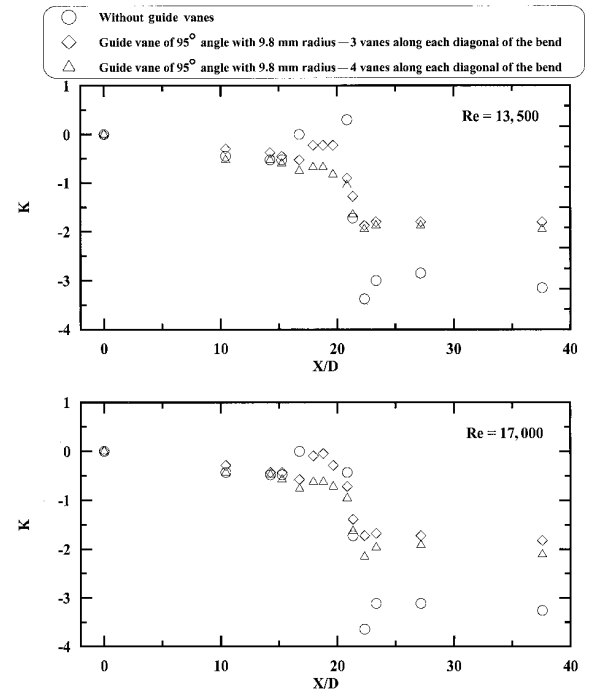


FIGURE 20

Outer surface pressure drop distribution in smooth square channel with guide vanes of 95° included angle and 9.8 mm radius.

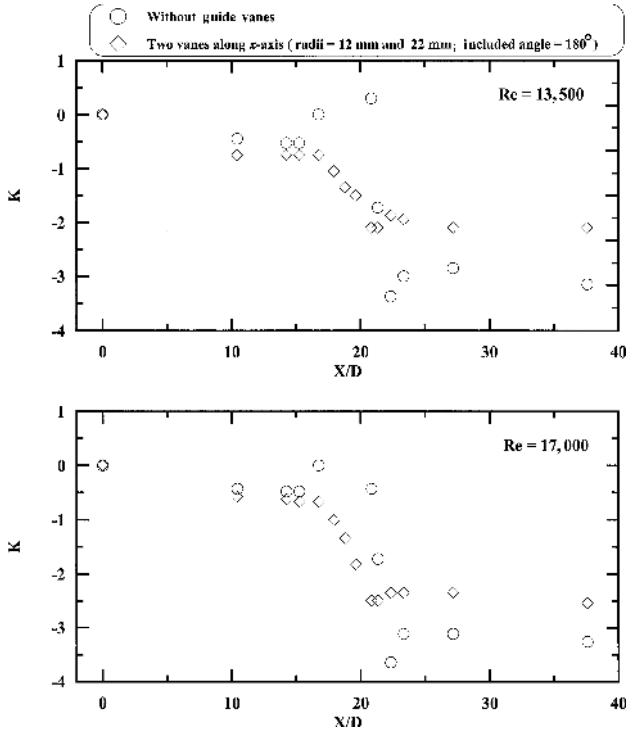


FIGURE 21

Outer surface pressure drop distribution in smooth square channel with 180° guide vanes of 12 and 22 mm radii.

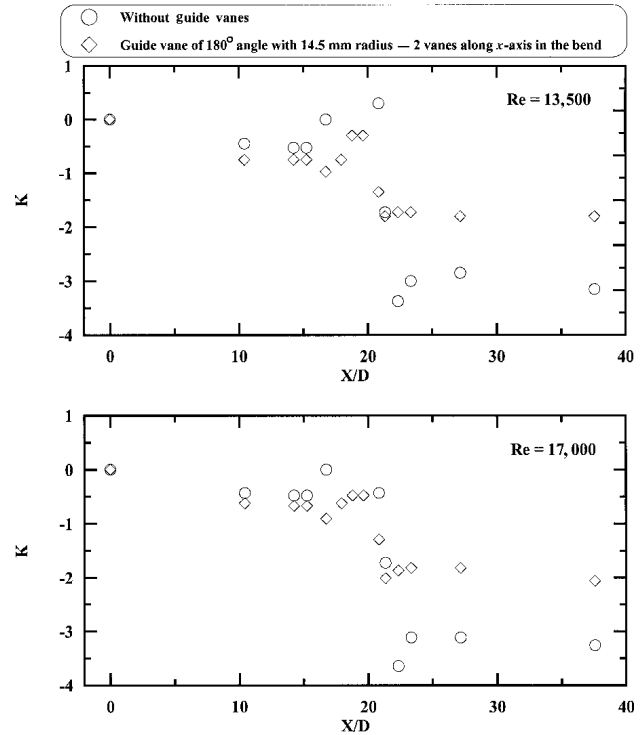


FIGURE 22

Outer surface pressure drop distribution in smooth square channel with 180° guide vane of 14.5 mm radius.

Figure 20 shows effect of the number of vanes with a radius of 9.8 mm and an included angle of 95° on the local pressure drop distribution. It can be observed that the overall pressure drop decreases in both 3-vane and 4-vane situations when compared with the no-guide vane situation by around 36–40%. The adverse gradient regions in the upstream of the bend ($X/D = 14.24$ – 17.94) and downstream of the bend ($X/D = 20.77$ –

22.27) are negligible in the presence of 4 vanes along each diagonal. However, adverse pressure gradients are observed in the upstream region of the bend ($X/D = 14.24$ – 17.94) when 3 guide vanes are placed along each diagonal. Figure 21 shows the effect of placing two guide vanes of 180° included angle with radii of curvature 12 mm and 22 mm which are equally spaced on the pressure drop distribution. The adverse pressure gradients in the

TABLE 3

Average Friction Factor Ratio for all the Smooth Channels Cases

Case	$\frac{f}{f(FD)}$ for $Re = 13,500$	Reduction in the overall pressure drop compared to the no-guide vane situation (%)	$\frac{f}{f(FD)}$ for $Re = 17,000$	Reduction in overall pressure drop compared to the no-guide vane situation (%)
No guide vane	3.0813	–	3.5189	–
1	2.2256	27.8	2.1309	39.4
2	2.1742	29.4	2.5351	28.0
3	2.40166	22.1	2.6056	26.0
4	3.38464	–9.9	3.9918	–13.4
5	4.7519	–54.2	5.7839	–64.4
6	2.8565	7.3	3.0115	14.4
7	1.9712	36.0	2.3502	34.6
8	1.871	39.3	1.9968	43.3
9	1.9712	36.0	2.2324	36.6
10	2.1742	29.4	2.6546	24.6
11	1.8195	41.0	2.1817	38.0

upstream and downstream corner of the bend have decreased considerably. However, the overall pressure drop decrease compared to that of no guide vane in the turn region is only around 28%. Figure 22 shows the effect of the placing equally spaced 180° extended vane and 290° extended vanes. It can be seen that the overall pressure drop decreases by inserting the extended guide vanes by 38–40%. Although the overall pressure drop

decreases drastically in this case, the adverse pressure gradients observed in the upstream zone and center of the bend ($X/D = 16.74-19.65$) are quite large.

The average friction factor ratio for all the cases covered in this study is summarized in the Table 3. Friction factor ratio observed at Reynolds number of 13,500 is consistently less than

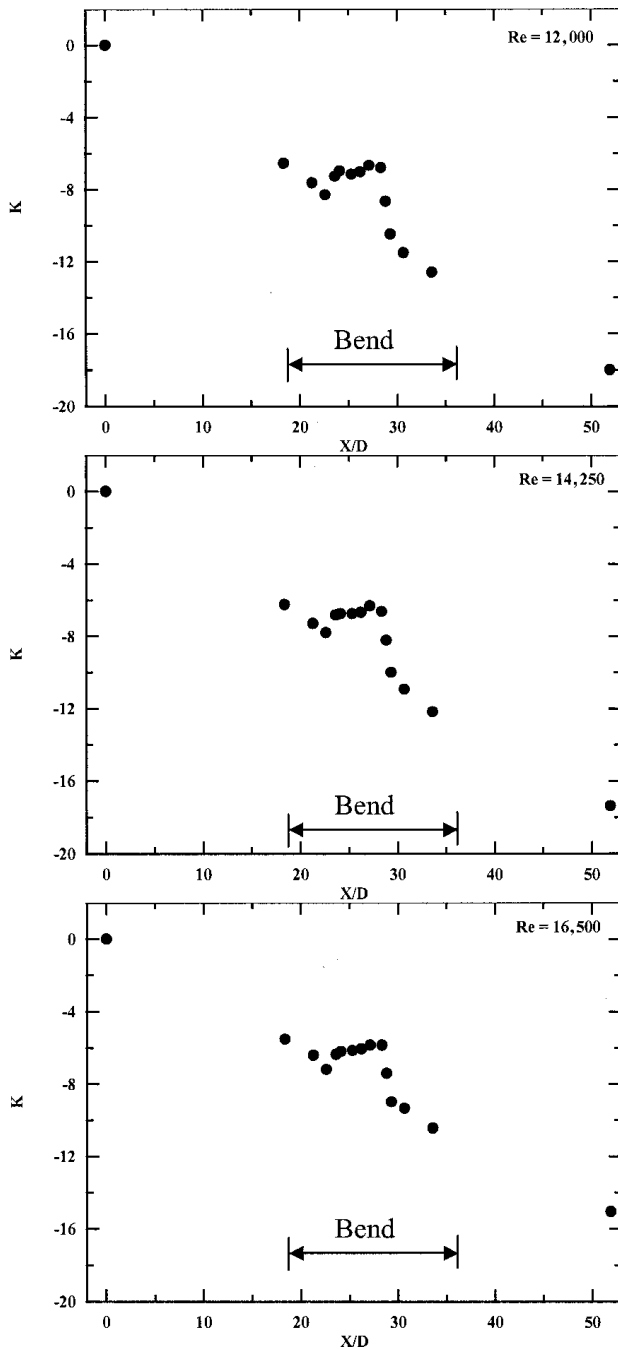


FIGURE 23

Outer surface pressure drop distribution in rib roughened channel with 180° bend without guide vane.

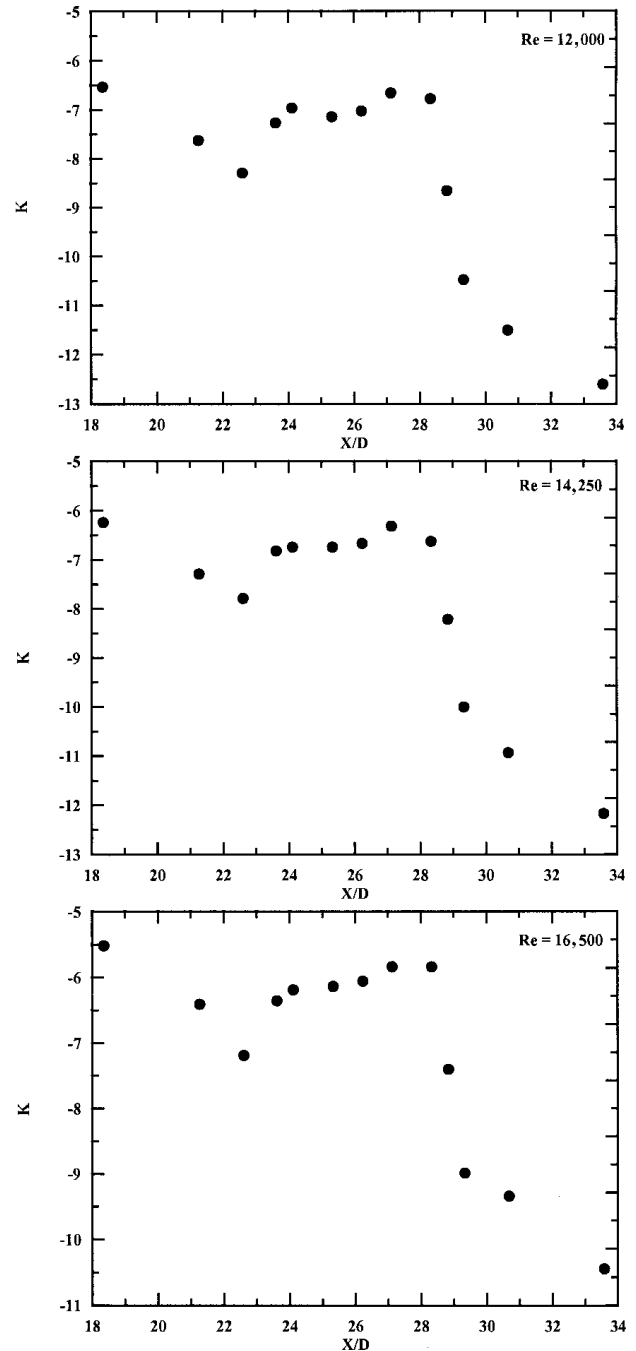


FIGURE 24

Outer surface pressure drop distribution in rib roughened channel with 180° bend without guide vane (enlarged view of bend zone).

that of Reynolds number 17,000. In general, there is a decrease in the overall pressure drop because of the presence of the guide vanes. Out of all the cases studied, Case 8 results in the least overall pressure drop. Cases 7, 9, and 11 are equally competitive as compared to Case 8. Although the decrease in the overall pressure drop in Case 10 situation is not comparable with that of

Case 8, Case 10 results in negligible adverse pressure gradients in the upstream and center zone of the bend.

Rib Roughened Square Channel with Sharp 180° Bend

Figure 23 shows the outer surface pressure drop distribution through a sharp 180° bend in the presence of the ribs for 3

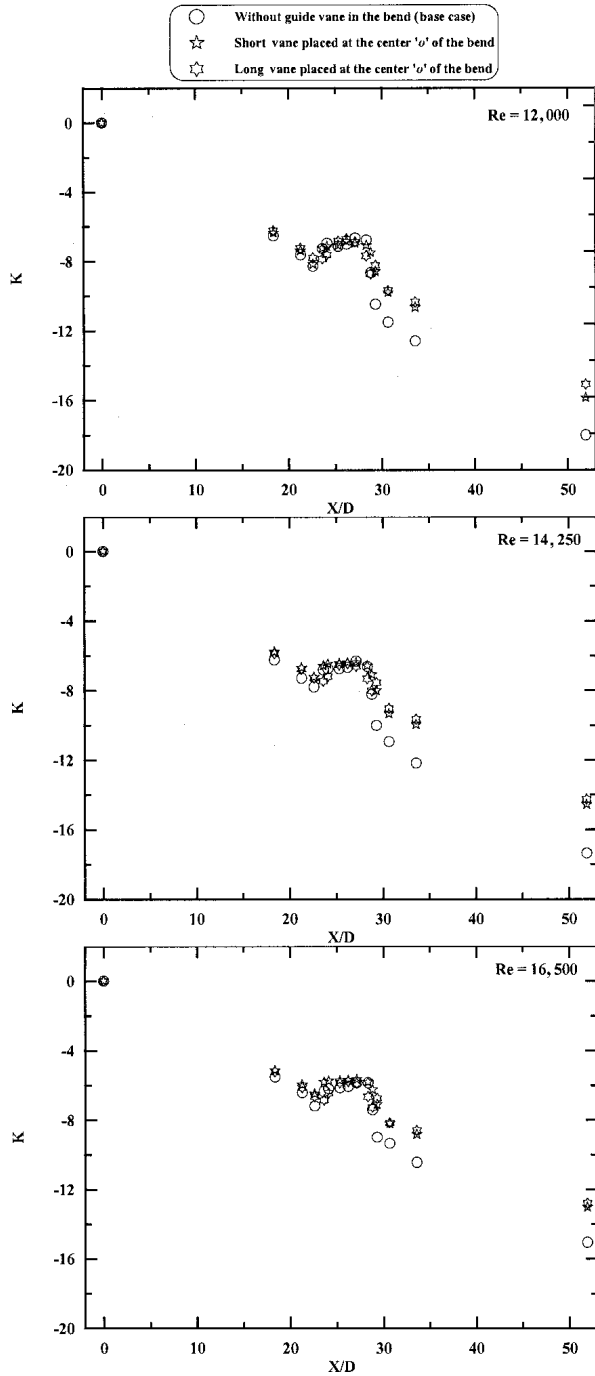


FIGURE 25

Outer surface pressure drop distribution in rib roughened channel with short guide vane and long guide vane at center of the bend.

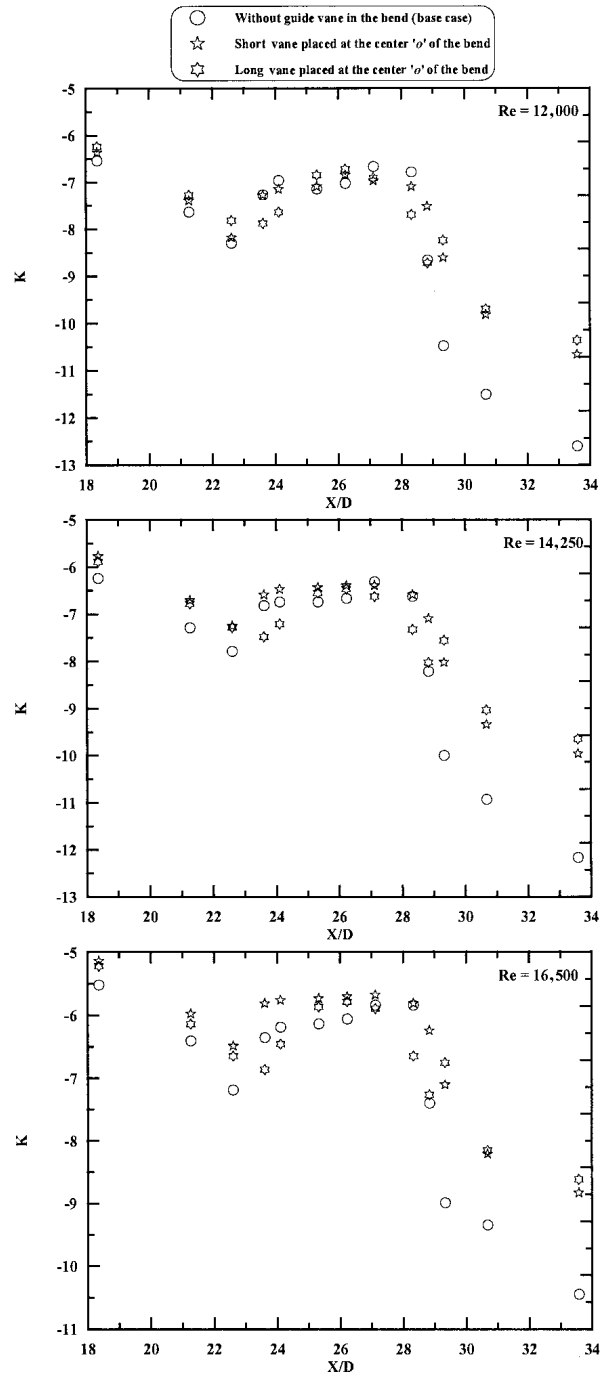


FIGURE 26

Outer surface pressure drop distribution in rib roughened channel with short guide vane and long guide vane at center of the bend (enlarged portion in the bend).

Reynolds numbers namely 12,000, 14,250, and 16,500. An enlarged view of only the bend zone pressure distribution ($X/D = 18-34$) is shown for improved clarity in Figure 24. Pressure drops favorably along the entrance channel ($X/D = 0-22.62$), then begins to rise in the vicinity of the upstream corner ($X/D =$

22.62–24.12), drops along the end wall ($X/D = 24.12-25.33$), rises again in the vicinity of the downstream corner ($X/D = 25.33-27.13$), drops largely to a minimum ($X/D = 27.13-29.34$), and then finally follows the favorable pressure drop in the downstream channel ($X/D = 29.34-50.95$). This pressure drop

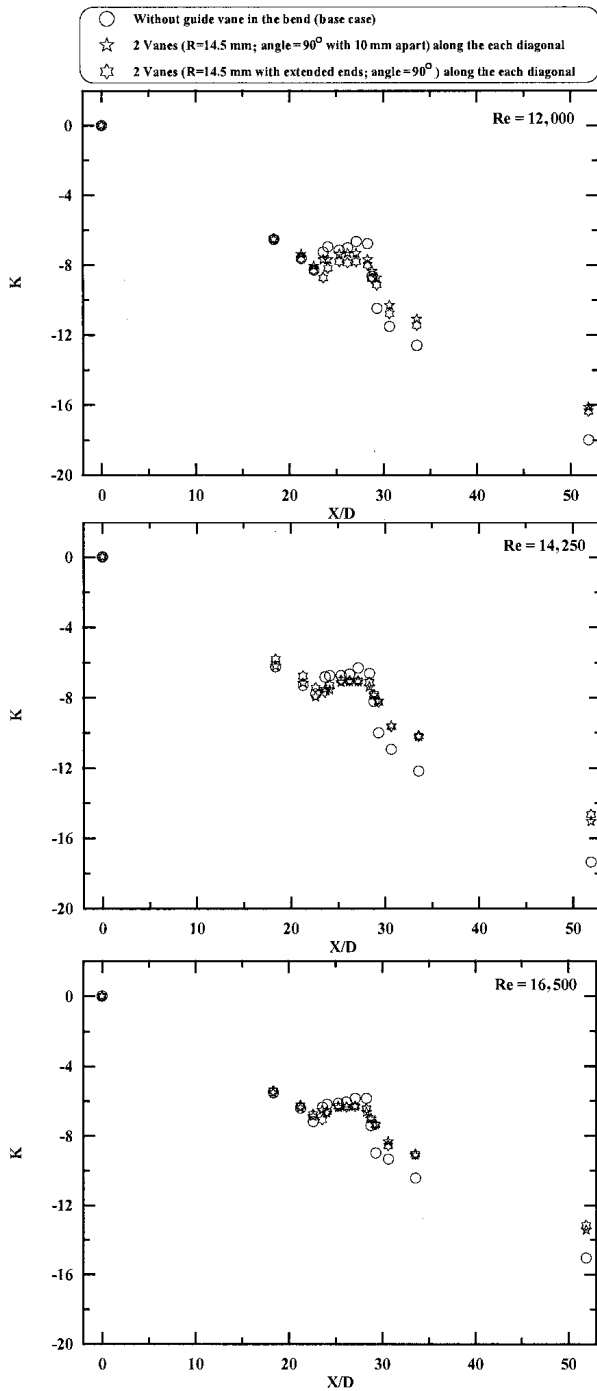


FIGURE 27

Outer surface pressure drop distribution in rib roughened channel with 90° vanes.

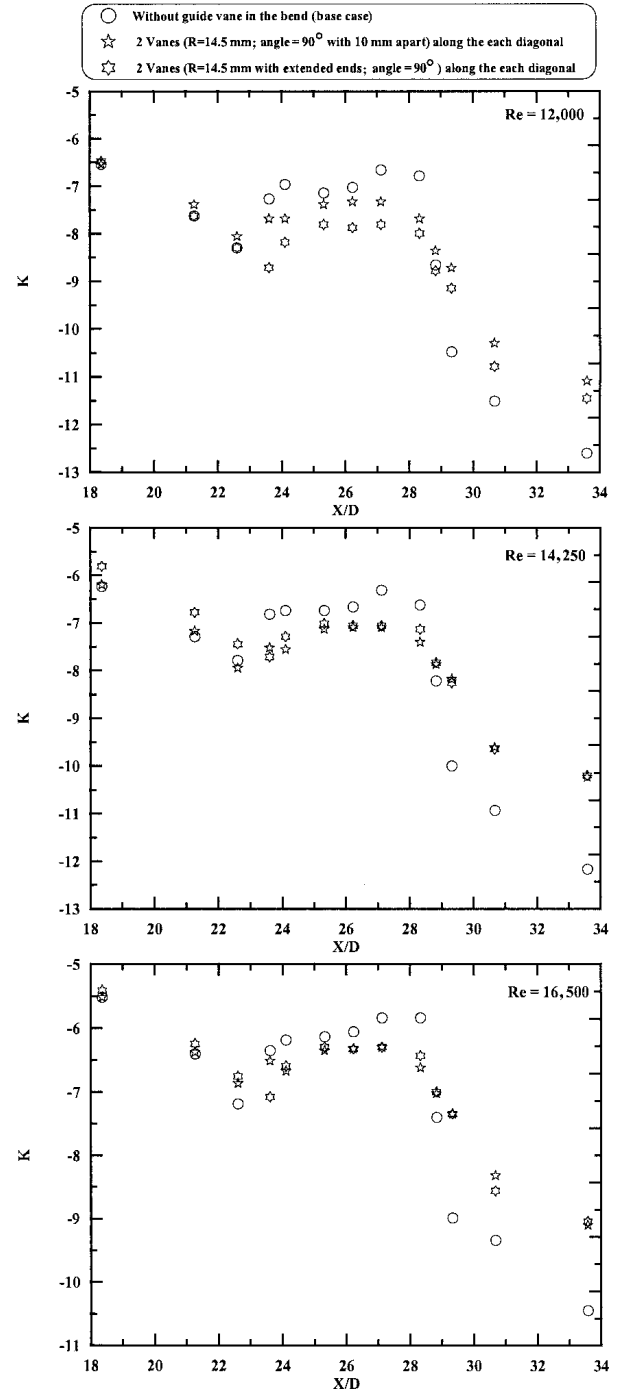


FIGURE 28

Outer surface pressure drop distribution in rib roughened channel with 90° vanes (enlarged View).

distribution indicates the several flow futures of the flow: large pressure drop in upstream and down stream channel because of ribs placed on the top and bottom surface, separated flow region in the upstream corner of the bend, acceleration and convergence of the upstream surface flow towards the divider tip, and

establishment of radially inward wall surface flow within and down stream of the turn.

Figure 25 shows the effect of the presence of the short guide vane and long guide vane placed in the sharp cornered 180° bend on the local pressure drop distribution. An enlarged view

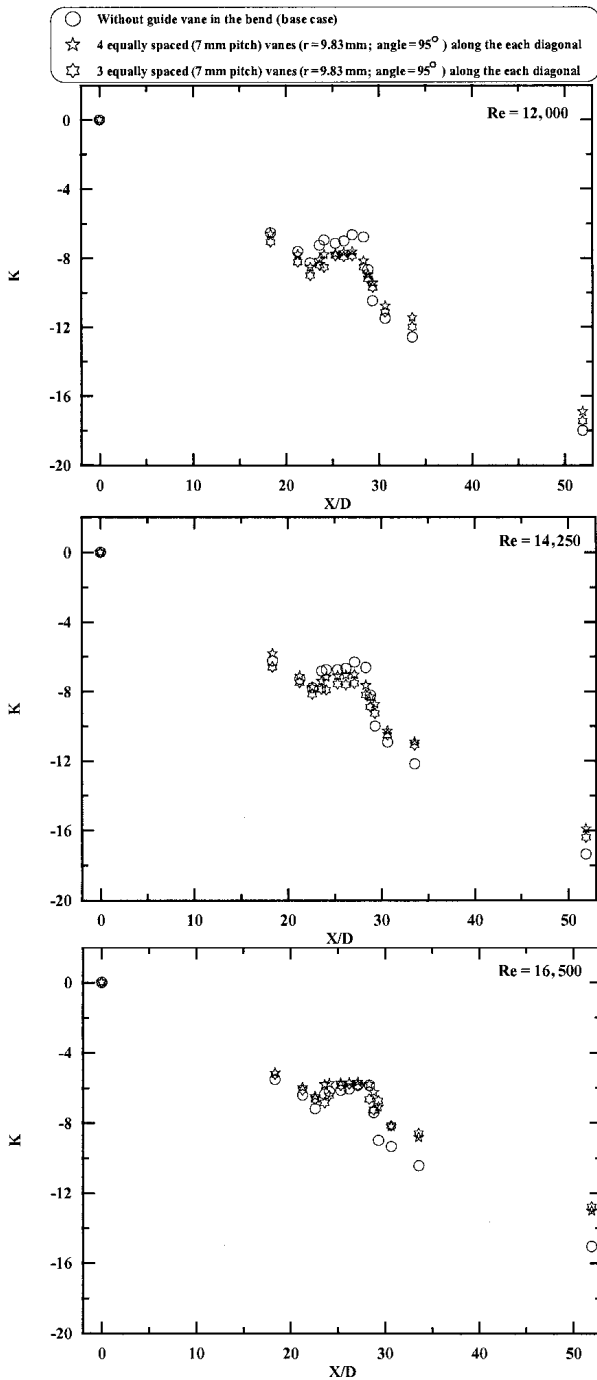


FIGURE 29

Outer surface pressure drop distribution in rib roughened channel with 95° vanes.

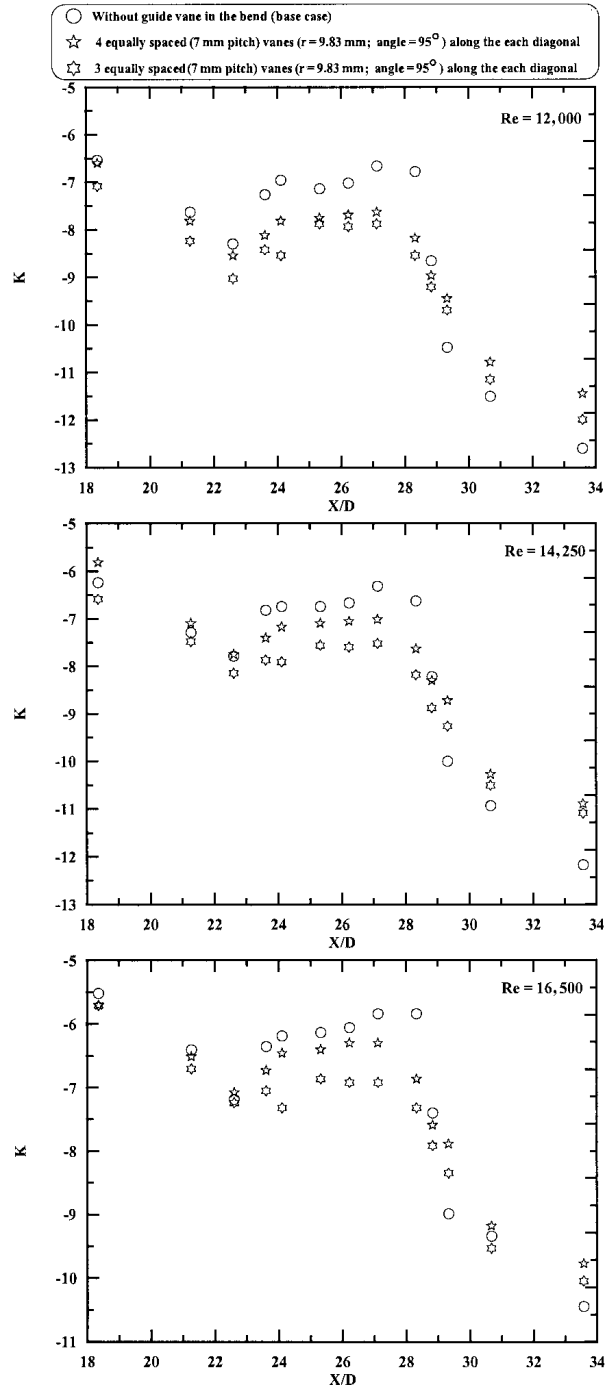


FIGURE 30

Outer surface pressure drop distribution in rib roughened channel with 95° vanes (enlarged View).

of only the bend zone pressure distribution ($X/D = 18-34$) is shown for improved clarity in Figure 26. Short guide vane and long guide vane placed at the center of the bend decreases the overall pressure drop by around 12–16% but has no effect on upstream and downstream adverse pressure gradients within the bend. Figure 27 shows the effect of the presence of equally

spaced multiple guide vanes (radius = 14.5 mm, included arc angle = 90°) placed in the sharp cornered 180° bend on the local pressure drop distribution. An enlarged view of only the bend zone pressure distribution ($X/D = 18-34$) is shown for improved clarity in Figure 28. In all the cases, the local pressure drop distribution is almost similar to that of the base case. The

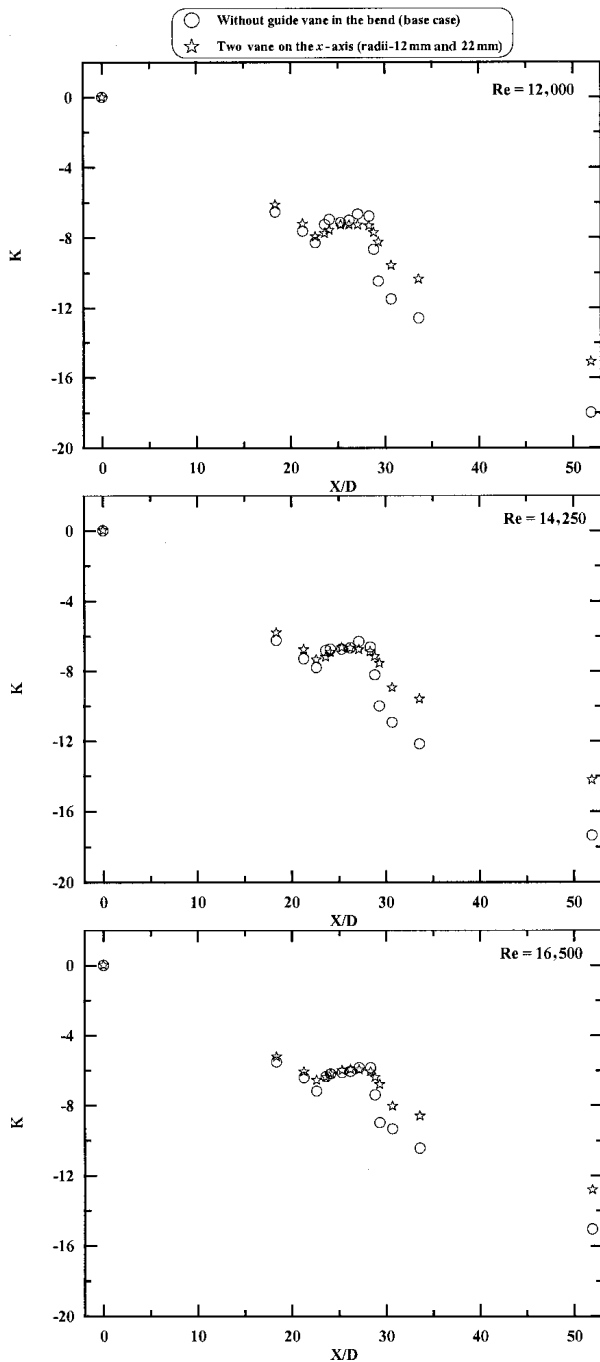


FIGURE 31

Outer surface pressure drop distribution in rib roughened channel with two 180° vanes.

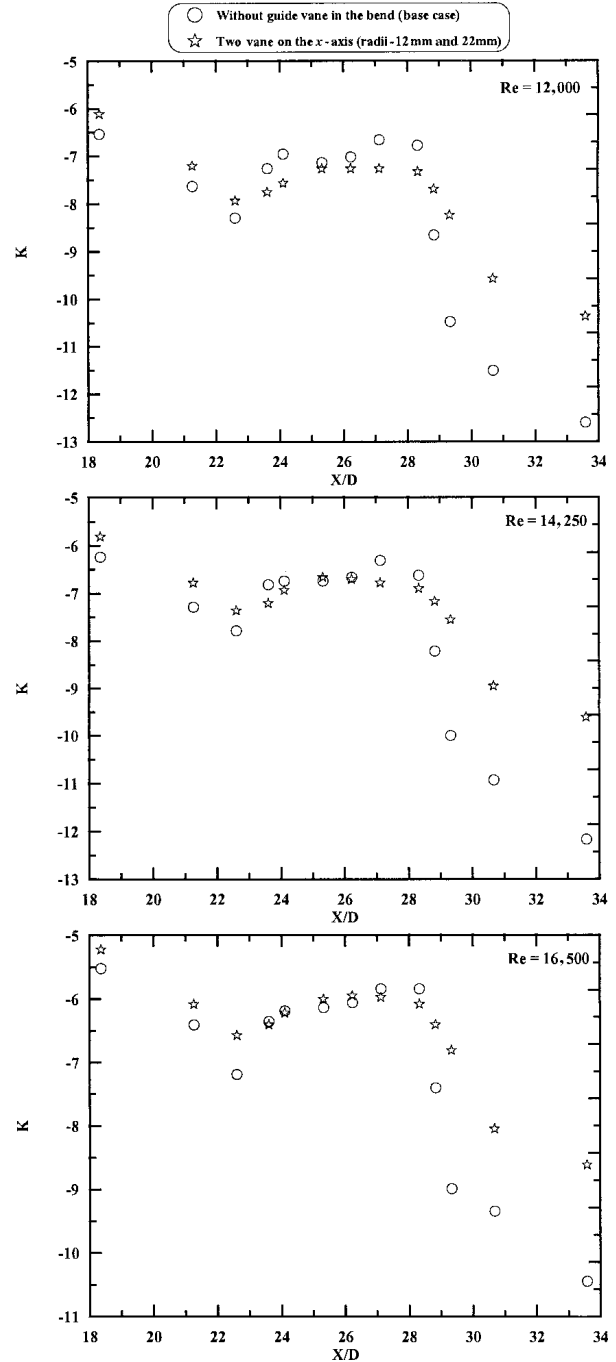


FIGURE 32

Outer surface pressure drop distribution in rib roughened channel with two 180° vanes (enlarged view of the bend).

TABLE 4
Average Friction Factor Ratio for all the Cases

Cases covered	$\frac{f}{f(FD)}$			Reduction in the overall pressure drop compared to the no-guide vane situation (%)		
	<i>Re</i>	<i>Re</i>	<i>Re</i>	<i>Re</i>	<i>Re</i>	<i>Re</i>
	12000	14250	16500	12000	14250	16500
1 Base Case	14.01206	14.46258	14.51671	—	—	—
2	12.34943	10.11473	12.56773	11.9	14.3	13.4
3	11.79625	12.27859	12.42901	15.8	15.1	14.4
4	12.5073	12.8814	12.8367	10.7	10.9	11.6
5	12.72946	12.56864	12.71661	9.2	13.1	12.4
6	12.96388	13.61651	13.72916	7.5	5.9	5.4
7	13.52015	13.89658	14.08868	3.5	3.9	3.0
8	11.73188	12.22231	12.35794	16.3	15.5	14.9

upstream and the downstream adverse pressure gradients consistently decrease because of the presence of the vanes in the bend resulting in a mild decrease in the overall pressure drop. Unextended vanes (Case 4) are more beneficial than that of extended vanes (Case 5).

Figure 29 shows the effect of the presence of equally spaced multiple guide vanes (radius = 9.8 mm, included arc angle = 95°, and distance between the vanes is 7 mm) placed in the sharp cornered 180° bend on the local pressure drop distribution. An enlarged view of only the bend zone pressure distribution ($X/D = 18-34$) is shown for improved clarity in Figure 30. In all the cases, the local pressure drop distribution is almost similar to that of the base case. The upstream and the downstream adverse pressure gradients consistently decrease because of the presence of the vanes in the bend. However, the presence of the vanes in the bend mildly improves the overall pressure drop by around 2–8%. Figure 31 shows the outer surface pressure drop distribution in the presence of 180° vanes of radii 12 mm and 22 mm. An enlarged view of only the bend zone pressure distribution ($X/D = 18-34$) is shown for improved clarity in Figure 32. The two guide vanes placed at the turn region of the bend result in the decrease of overall pressure drop by around 15–16%.

The average friction factor ratio for all the cases covered in rib roughened channels is summarized in the Table 4. In general, there is a decrease in the overall pressure drop because of the presence of the guide vanes. Out of all the cases studied, Cases 3 and 8 result in the least overall pressure drop by around 14–16%. Cases 2 and 5 are also equally competitive as compared to Cases 3 and 8.

CONCLUSIONS

An experimental investigation is conducted to investigate the pressure drop distribution in smooth and rib roughened square channel with round ended 180° bend in the presence of single

and multiple guide vanes. The sharp 180° bend is obtained by dividing a rectangular passage into two channels using a divider wall with a round ended tip at the location where the flow negotiates the turn.

Conclusions from the local and overall pressure drop measurements in a smooth square channel with a sharp 180° bend are as follows

- Short and long guide vanes placed at the center of the bend result in a decrease of around 28% overall pressure drop compared to that of the no guide vane situation.
- Overall pressure drop is sensitive to the location at which the short and long guide vane is placed within the bend region. Increase in the overall pressure drop is observed when the guide vane is shifted towards the upstream and downstream surface. However, shifting the guide vane towards the divider tip and end surface decreases the overall pressure drop by around 22% and 14%, respectively.
- 90° multiple vanes and 90° extended multiple guide vanes result in the decrease of overall pressure by around 36–44%.
- 180° extended multiple guide vanes result in the decrease of overall pressure drop by only 25%. However, adverse pressure gradients in the upstream and downstream of the bend are negligibly small in the case of 180° extended multiple guide vanes.

Conclusions from the local and overall pressure drop measurements in a rib roughened square channel with sharp 180° bend are as follows:

- Pressure drop contributed by the rib roughened upstream and downstream passages is considerably large compared to the pressure drop contributed by the bend region.

- Maximum decrease of 15–16% in the overall pressure drop is observed in case of long guide vane located at the center of the bend and multiple 180° extended guide vanes.

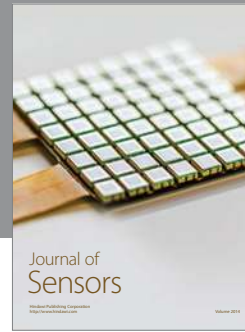
The experimental results obtained in this study are likely to be useful to the designer of gas turbine blade internal coolant passages. The overall friction factor behavior presented would result in the more accurate prediction of the coolant flow rate which is an essential prerequisite for the estimation of the heat transfer rate. The detailed pressure distributions are also of fundamental interest since they reveal several important flow characteristics, like the zones where separated flow regions and locally accelerating flows are likely to occur.

NOMENCLATURE

D	Hydraulic diameter (m)
e	Rib height (m)
f	Average friction factor (Eq. 2)
$f(FD)$	Fully developed friction factor in smooth circular tubes
g	Acceleration due to gravity (m/s^2)
K	Non-dimensional pressure drop (Eq. 1)
L	Length of the test section (m)
P	Rib pitch (m)
P_{in}	Static pressure at channel entrance (Pa)
P_X	Static pressure at an axial distance from channel entrance (Pa)
P_{ex}	Static pressure at the channel exit (Pa)
Re	Reynolds number ($\rho U D / \mu$)
U	Average velocity in flow channel (m/s)
W	Divider wall thickness (m)
X	Axial distance from the channel entrance (m)
ρ	Density of water (kg/m^3)
μ	Dynamic viscosity of water (Pa.s)

REFERENCES

- Ekkad, S., and Han, J. C. 1997. Detailed heat transfer distributions in two pass square channels with rib turbulators. *International Journal of Heat and Mass Transfer* 40:2525–2537.
- Han, J. C., and Zhang, P. 1989. Pressure loss distribution in three pass rectangular channels with rib turbulators. *ASME Journal of Turbomachinery* 111:515–521.
- Kline, S. J., and McLintock, F. A. 1953. Describing uncertainties in single sample experiments. *Mechanical Engineering* 75: 3–8.
- Kwak, D., Chang, J. L. C., Shanks, S. P., and Chakravarthy, S. R. 1986. A three-dimensional incompressible navier-stokes flow solver using primitive variables. *AIAA Journal* 24(3):390–396.
- Liou, T. M., and Chen, C. C. 1999. Fluid flow in a 180° sharp turning duct with different divider thicknesses. *ASME Journal of Turbomachinery* 121:569–576.
- Metzger, D. E., Plevich, C. W., and Fan, C. S. 1984. Pressure loss through sharp 180° turns in smooth rectangular channels. *ASME Journal of Engineering for Gas Turbines and Power* 106:677–681.
- Metzger, D. E., and Plevich, C. W. 1990. Effects of turn region treatments on pressure loss through sharp 180° bends. *Proceedings of Third International Symposium on Transport Phenomena and Dynamics of Rotating Machinery, ISROMAC-3*, 301–312.
- Ratna Rao, D. V., Sarat Babu, C., and Prabhu, S. V. Effect of turn region treatments on the pressure loss distribution in a smooth square channel with sharp 180° bend. *International Journal of Rotating Machinery*, forthcoming.
- Son, S. Y., Kihm, K. D., and Han, J. C. 2002. PIV flow measurements for heat transfer characterization in two pass square channels with smooth and 90° ribbed walls. *International Journal of Heat and Mass Transfer*, 45:4809–4822.
- Taylor, J. R. 1997. *An Introduction to Error Analysis—The Study of Uncertainties in Physical Measurements*, 2nd ed., University Science Books, Sausalito, CA.



Hindawi

Submit your manuscripts at
<http://www.hindawi.com>

